

that will allow the prediction and optimization of concentrator geometry, part location and braze thermal cycles so that this method is extendable to other part configurations.

Modeling of Energy Flux Using Ray Tracing

One of the first researchers to analyze and exploit the principles of nonimaging optical concentration was Mendenhall, who in 1911 described the use of a wedge-shaped optical concentrator (Ref. 6). Many subsequent studies have been undertaken to apply nonimaging concentrators for such applications as solar collectors, infrared and optical detectors, and optical pumping (Ref. 7). In this work, a methodology for the application of the principles of nonimaging optics and computational ray tracing to the understanding and design of high-performance laser weld joints (Refs. 8–11) was extended and enhanced for the prediction and optimization of the brazing of small-diameter tubing.

Two 3-D models were created using the *OptiCad* optical ray-tracing software package. Two simple energy concentration devices, a wedge and a cone, were modeled along with a two-piece braze joint assembly and a heat source, as shown in Figs. 1 and 2. The size, location and orientation of each component were adjustable within the model. The model also can represent the heat source as either a distributed collimated beam or a localized focused beam of specified divergence and energy. The heat sources are represented by a distribution of rays, each carrying a specified amount of energy that is deposited within the model upon surfaces that the ray impinges. These surfaces are made up of an absorptive feature that records the location

of the ray impingement and amount of energy deposited and a reflective feature that redirects the unabsorbed remainder of energy back into the 3-D model.

The model employs nonsequential ray tracing that allows a ray to impact any surface in any order. As the rays propagate throughout the model, they give up energy until they lose 99% of their original energy and are then terminated. To obtain an adequate statistical representation of energy propagation, typically 10,000 rays were traced over a region of space defined by the distributed heat source object. The reflective surfaces of the copper concentrators were defined to have a reflective coefficient of 98%. No energy absorption is recorded for the reflector walls. The tube sections were defined to possess an energy absorption value of 35%, typical for Nd:YAG radiation on stainless steel, and, conversely, a reflective value of 65% (Ref. 12). Energy impinging upon the tube section can reflect back onto the walls and back onto the tube, allowing multiple absorption opportunities. Beneath the partially reflective walls of the tube geometry lies a mesh of absorptive detector units, which record the location and intensity of energy deposited for all impinging rays. Braze preform geometry was not considered within this model. The effects of angle-dependent absorption, beam polarization and scattering were also not considered (Ref. 11). Energy output was displayed by graphing the absorptive mesh data, which is also used to calculate total energy absorption by the tube and determine the uniformity of tube surface illumination.

The models were run on a laptop computer, and the tracing of 10,000 rays required approximately 2 min of run time. The total energy input into the sys-

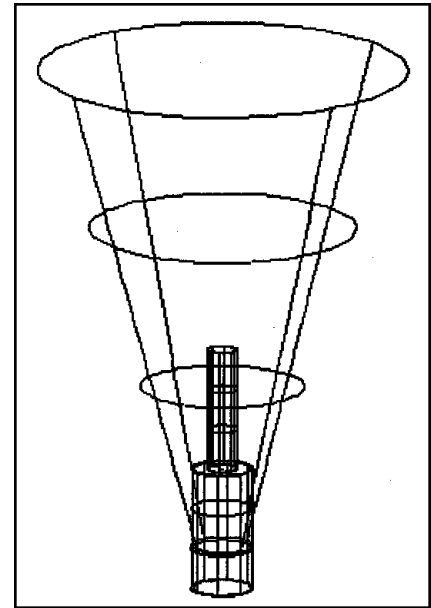


Fig. 1 — Model of conical concentrator showing part placement within concentrator.

tem was distributed evenly among the number of rays specified. Variations in wedge and cone geometry, laser beam size and location, and tube joint location were made to develop a qualitative appreciation for the interaction of these parameters and a quantitative output of energy absorption versus position of the braze joint. The use of these ray-tracing models provided insight and direction for experimental trials and input of the illumination data into the heat flow models.

Experimental Procedure

The laser and test chamber are shown in Fig. 3. A Raytheon SS-500, 400-W av-

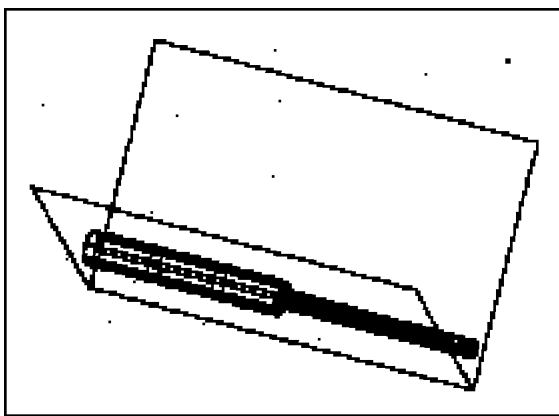


Fig. 2 — Model of wedge concentrator showing part placement within concentrator.

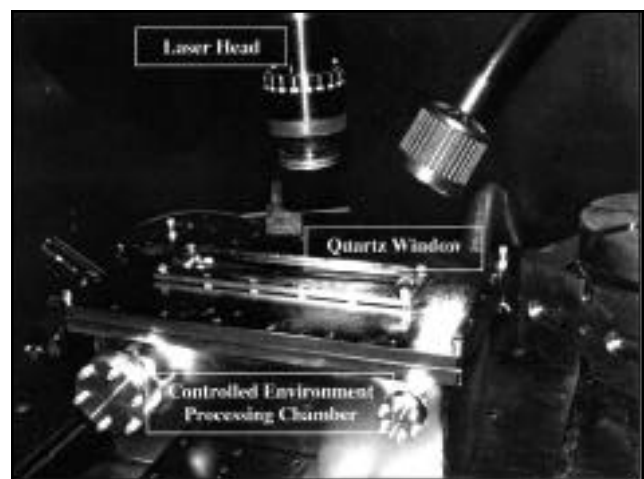


Fig. 3 — Braze processing chamber and its relative position with respect to the laser.

